

The Non-Stationary Case of Maxwell-Garnett: Growth of Nanomaterials (2D gold flakes) in Solutions

P. Natarajan, ^{[a], ‡} A. Shalabny, ^{[a], ‡} S. Sadhujan, ^[a] A. Idlibi, ^[a] M. Y. Bashouti ^{[a],[b],*}

[a] Department of Solar Energy and Environmental Physics, Swiss Institute for Dryland Environmental and Energy Research, J. Blaustein Institutes for Desert Research, Ben-Gurion University of the Negev, Midreshet Ben-Gurion 8499000, Israel.

[b] The IlSe-Katz Institute for Nanoscale Science & Technology, Ben-Gurion University of the Negev, Beersheva, 8410501, Israel.

‡ P Natarajan and A Shalabny are equally contributed.

SI-1: Simulation of the dielectric constant

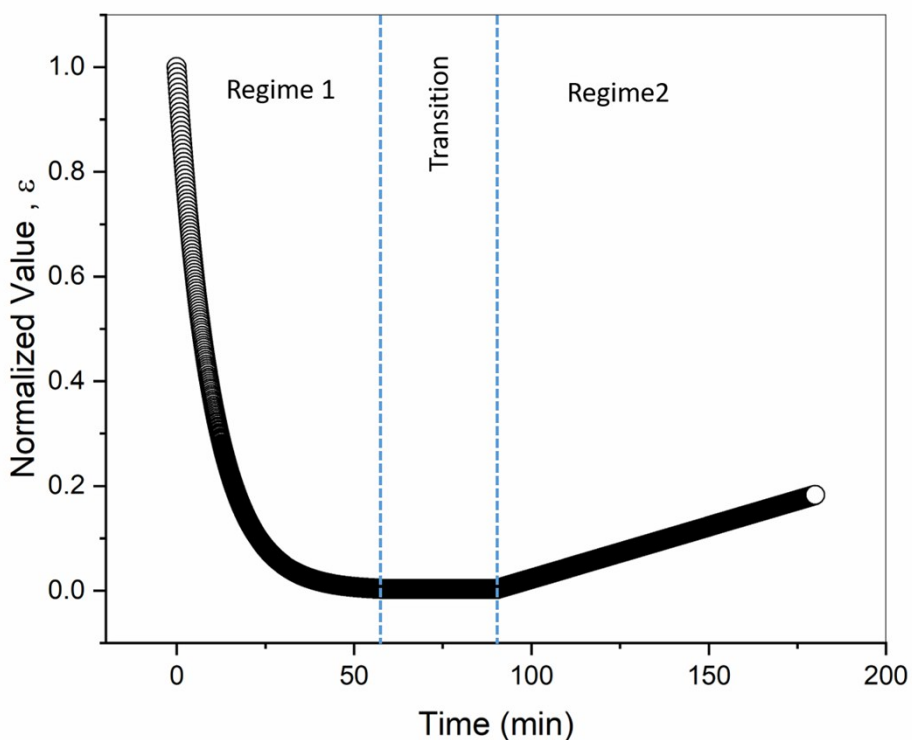


Figure SI-1. Simulation of the normalized dielectric constant based on the optical observation. Three regimes were identified: 0-90, regime 1, the transition from 60-90min then from 90 to 180min.

SI-1: Metal-ion-ethylene glycol interaction: To get more information regards the 367nm peak, we subtract the Au-Cl spectra with ethylene glycol from the polymer solution (with Au-Cl & EG) and following the change in 367nm along the reaction. We note that a negligible change appears only after 120 min while 322nm peak was decreasing rapidly [Ö. Dag, O. Samarskaya, N. Coombs, G. A. Ozin, *J. Mater. Chem.* **2003**, *13*, 328–334]. Thus, 367nm peak major contributor is gold ions interaction with ethylene glycol [see Fig SI-1].

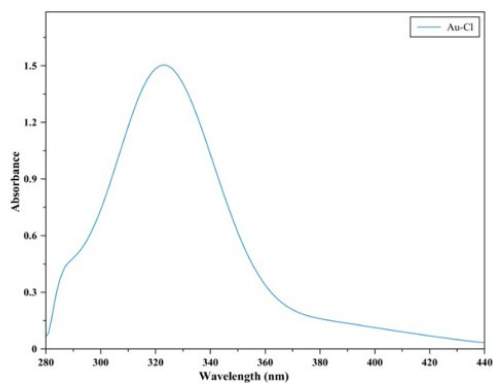


Fig SI-1: Absorbance of the AuCl_4^- with ethylene-glycol.

The Au(III) species exist in a form of $[\text{AuCl}_4]^-$. The 322nm peak is related to the Au-Cl ligand. In addition, when the oxidation of PANI finish ($t > 90\text{min}$), then the thermal reduction occurring between the $[\text{AuCl}_4]^-$ complex with ethylene glycol become the controlling mechanism.

SI-2: X-Ray of the 2D monocrystalline gold flakes.

As can be seen from SI-2, the obtained gold flakes show a perfect crystallinity with [111] facets.

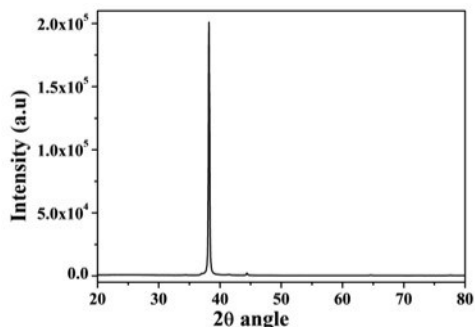


Figure SI-2: XRD of the 2D- monocrystalline gold synthesized in EG solution.

SI-3: The Mechanism

The summary of the mechanism is shown in the following figure SI-3. The two regimes with the relevant important feature are illustrated: (i) two main regimes (0-90min) with relevant two phases (0-60min) and (60-90min) and the (ii) kinetic rates and the PAOS along the different regimes.

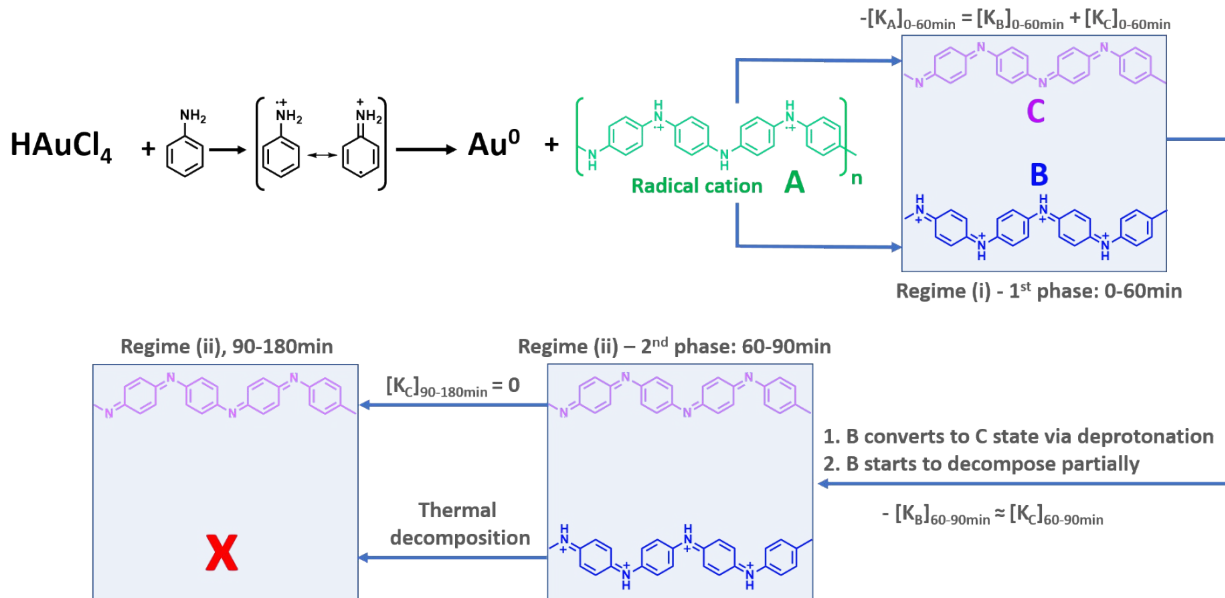


Figure SI-3: Schematic illustration of PAOS formation, the molecular changes that occur, and the two main reaction regimes, i.e. 0-90min, and 90-180min.

SI-4. Error bars Calculations: The error in the absorbance [as an example] was calculated by equation 1.

$$\text{equation 1: } \text{error}\% = \frac{X1 - X2}{\min(X1, X2)} * 100\%$$

Where X1 & X2 represent the real value and fitting values respectively. The error between the fitting and real value for each time separately give us the different error percentage as shown in table S1.

Table S1I. Calculated error between deconvolution peaks values extracted by modified and raw spectra

Parameter	Polymer A	Protonation Peak	Polymer C	Polymer B
Error in the width (%)	0	3.99	0.49	5.3
Error in the Wavelength (%)	0.01	2.93	0.34	0.07
Error in the Absorbance (%)	0.48	13.4	5	7.53

As shown the errors are negligible and may indicate that our substitution method can be used to deconvolution properly the UV-Vis spectra [Table SI2). This is being applied for all the spectra along the reaction time. As an example, we show the error in the absorbance from 0 to 180min. As shown, the error bars change with the time, this is due to the change in the solution composition. With time different shapes

of gold appear leading to increase the light scattering inside the solution, thus, the error in the measurement increase.

Table SI2. Calculated error between sum values extracted by deconvolution and real values

Time [min]	Error %
0	2.67
5	2.12
10	1.64
20	3.23
30	3.42
45	4.95
60	8.15
75	10.29
90	11.72
110	6.68
120	7.00
150	11.20
180	16.60

With the same principle, we check the full width at half-maximum (fwhm) for all the PAOS and Au. We found that the fwhm was identical ($\pm 5\%$) for the B and C states of the PAOS over the reaction course (66 ± 3 nm), while the A form exhibited a smaller fwhm due to polymer homogeneity (48 ± 1 nm). [M. Fujiki, H. Nakashima, S. Toyoda, J. Koe in Materials-chirality (Eds.: M. M. Green, R. J. M. Nolte, E. W. Meijer), Wiley, Hoboken, NJ, 2003, p. 209–280]

Mass conservation: As shown in figure SI-3, the total polymer mass start to decrease after 60 min due to the decomposition of polymer B as discussed in the paper. The total mass has calculated by sum all the PAOS since all the oxidized states has almost same structure and molecular weight, which make this approximation logical.

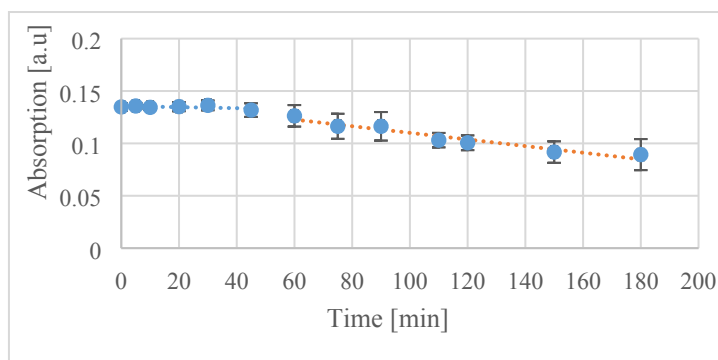


Figure SI-4: Mass reservation: the sum of absorption for all PAOS

SI-5. AFM study: Figure SI-5 shows AFM images in the two regimes. In the first phase of regime 1, Figure SI-5a show separated seeds which start to agglomerate in the second phase (SI-5b). Interestingly, in this phase we can see the PAOS (B and C) around the agglomerated nanoparticles (light blue color around the

gold which is in red). Subsequently, the state C remain and leads to flake structure i.e. the nanoparticles decompose to produce 2D flakes (SI-5c).

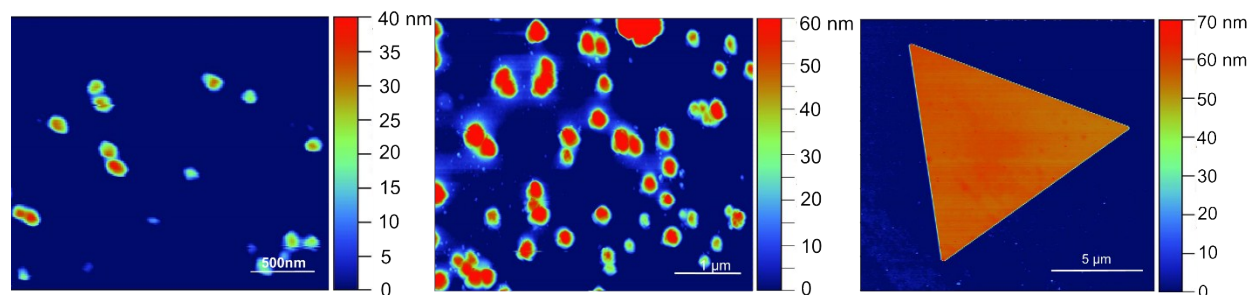


Figure SI-5: AFM images of the samples at: (a) 40 min, i.e. phase 1, (b) 60 min, i.e., phase 2, and (c) 180 min, i.e. the second regime.

SI-5. Adding additional surfactant (Cetyltrimethylammonium bromide, CTAB) and replacing ethylene glycol with water: In ethylene glycol solvent (EG), the Au seeds are randomly formed even after complete oxidation of polyaniline. These seeds aren't completely capped by polyaniline to form 2D Au microplates. Therefore, it leads to form Au particles with different shape. To study the effect of EG, we carried out the reactions in both EG and water solvents with CTAB (CTAB: HAuCl_4 (2:1)). In both case, CTAB used to kinetically control the reaction and aniline primarily acts as reducing agent. Figure SI-5a shows that the sample had small percentage (~5%) of particles in EG solvent. This indicated that the growth is not completely controlled via CTAB and polyaniline due to EG. On the other hand, in water, since there is no EG, the reaction is directly depending on the aniline assisted reduction of $[\text{AuCl}_4]^-$, and the growth completely controlled by CTAB and oxidized aniline, which yielded 2D Au microplates (Figure SI-5b) with no Au particles (less than 1%). Similar results also found for Cetyltrimethylammonium chloride (CTAC). Thus, adding additional surfactant and replacing EG are facilitating to grow more 2D Au plates with less or no Au particles.

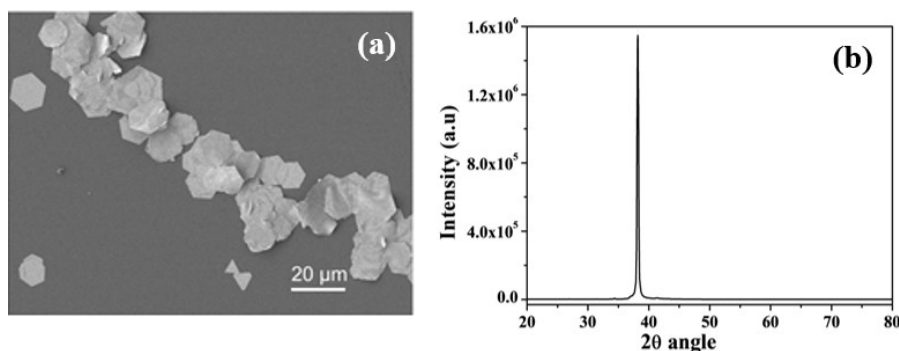


Figure SI-6: (a) SEM images of the samples synthesized in water, and (b) XRD of the gold flakes shows perfect [111] crystallinity.

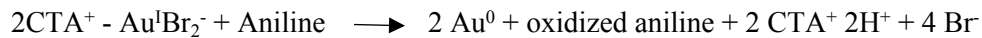
Chemical Reaction of CTAB:

The CTAB forms a completely different complex when adding to $[\text{AuCl}_4]^-$ ions. The Br^- ions of CTAB replaces the Cl in $[\text{AuCl}_4]^-$ and forms $[\text{AuBr}_4]^-$ CTA complex as follows.



Yellow - orange yellow color in the solution.

First reduction: Au III to Au I



This $\text{CTA}^+[\text{AuBr}_4]^-$ complex is more stable when compare to $[\text{AuCl}_4]^-$ and follows different reduction reaction pathway. So, we cannot apply the same model for CTAB assisted growth. However, addition of CTAB kinetically controls the reaction which yields more 2D Au. (The t_1 and t_2 will be different and the change is not predictable). However, the time-dependent may remain only if we could recognize the different regimes.